Hindawi
Journal of Nanotechnology
Volume 2021, Article ID 5611434, 15 pages
https://doi.org/10.1155/2021/5611434

Research Article

Optimization, Characterization, and Antibacterial Activity of Copper Nanoparticles Synthesized Using *Senna didymobotrya* Root Extract

Bernard Otieno Sadia,[1,2] **Jackson Kiplagat Cherutoi**,[1] **and Cleophas Mecha Achisa**[3]

[1]*Department of Chemistry and Biochemistry, School of Sciences and Aerospace Studies, Moi University, P.O. Box 3900-30100, Eldoret, Kenya*
[2]*Africa Centre of Excellence II in Phytochemicals,Textile and Renewable Energy (ACE II PTRE), Moi University, P.O. Box 3900-30100, Eldoret, Kenya*
[3]*Department of Chemical and Process Engineering, School of Engineering, Moi University, P.O. Box 3900-30100, Eldoret, Kenya*

Correspondence should be addressed to Bernard Otieno Sadia; benardsadia@gmail.com

Received 11 August 2021; Revised 3 October 2021; Accepted 8 October 2021; Published 15 October 2021

Academic Editor: Brajesh Kumar

The economic burden and high mortality associated with multidrug-resistant bacteria is a major public health concern. Biosynthesized copper nanoparticles (CuNPs) could be a potential alternative to combat bacterial resistance to conventional medicine. This study for the first time aimed at optimizing the synthesis conditions (concentration of copper ions, temperature, and pH) to obtain the smallest size of CuNPs, characterizing and testing the antibacterial efficacy of CuNPs prepared from *Senna didymobotrya* (*S. didymobotrya*) roots. Extraction was done by the Soxhlet method using methanol as the solvent. Gas chromatography-mass spectrometry (GC-MS) analysis was performed to identify compounds in *S. didymobotrya* root extracts. Box–Behnken design was used to obtain optimal synthesis conditions as determined using a particle analyzer. Characterization was done using ultraviolet-visible (UV-Vis), particle size analyzer, X-ray diffraction, zeta potentiometer, and Fourier transform infrared (FT-IR). Bioassay was conducted using the Kirby–Bauer disk diffusion susceptibility test. The major compounds identified by GC-MS in reference to the NIST library were benzoic acid, thymol, N-benzyl-2-phenethylamine, benzaldehyde, vanillin, phenylacetic acid, and benzothiazole. UV-Vis spectrum showed a characteristic peak at 570 nm indicating the formation of CuNPs. The optimum synthesis conditions were temperature of 80°C, pH 3.0, and copper ion concentration of 0.0125 M. The FT-IR spectrum showed absorptions in the range 3500–3400 cm^{-1} (N-H stretch), 3400–2400 cm^{-1} (O-H stretch), and 988–830 cm^{-1} (C-H bend) and peak at 1612 cm^{-1} (C=C stretch), and 1271 cm^{-1} (C-O bend). Cu nanoparticle sizes were 5.55–63.60 nm. The zeta potential value was −69.4 mV indicating that they were stable. The biosynthesized nanoparticles exhibited significant antimicrobial activity on *Escherichia coli* and *Staphylococcus aureus* with the zone of inhibition diameters of 26.00 ± 0.58 mm and 30.00 ± 0.58 mm compared to amoxicillin clavulanate (standard) with inhibition diameters of 20 ± 0.58 mm and 28.00 ± 0.58 mm, respectively.

1. Introduction

Nanotechnology is of great scientific interest due to its wide application in pharmaceutical products, electronics, biotechnology, and medicine [1, 2]. Nanoparticles are solid particles with sizes approximately extending from 1 nm to 100 nm in length in at least one dimension [3]. Their application in the field of biotechnology has grown because of their comparable size range scale to biomolecules and their versatile properties that can be controlled using the method used for their biosynthesis [4]. Copper nanoparticle (CuNP) is one of the most common nanoparticles utilized in medicine. They have been synthesized using both physical and chemical methods [4]. Physical methods experience low

production of nanoparticles and high energy consumption to maintain high temperature and pressure utilized during the synthesis process. Chemical methods are known to use noxious precursor chemicals, harmful by-products, and uses toxic solvents [5, 6].

Due to the limitations of physical and chemical methods of CuNPs synthesis, biological methods have been developed. These use bacteria, algae, fungi, plants, and plant products. The biological method of synthesis of the copper nanoparticle is considered a bottom-up technique, where oxidation or reduction is the main reaction that occurs during the production of nanoparticles [7]. Currently, the use of phytochemicals in the synthesis of nanoparticles is being explored as such nanoparticles are friendly both to the environment and humans [8]. Biosynthesized inorganic nanoparticles can offer solutions to the emergence of multidrug-resistant microbes. This can act as substitutes to the traditional organic agents that have limited application due to the high rate of decomposition and low heat resistance. The unique chemical and physical properties, low-cost preparation, surface-to-volume ratio, and low toxicity make CuNPs command a superior position as gas sensors, photocatalysts, dye absorbents, antioxidant, antimicrobial, antimalarial, and antitumor agents in comparison to nanoparticles prepared from gold, zinc, iron, and silver compounds [2, 9–13].

Senna didymobotrya (Fresen) Irwin & Barneby (Synonym: *Cassia didymobotrya* Fresen.), a plant from the genus *Senna* and family Fabaceae has been used by different ethnic communities worldwide [14–16]. In Kenya, it is used to treat malaria, fungal and bacterial infections, hypertension, haemorrhoids, sickle cell anaemia, a range of diseases affecting women such as inflammation of fallopian tubes, fibroids, and backache, stimulate lactation, and induce uterine contraction and abortion [17–26]. Preceding authors reported that aqueous and organic extracts and fractions of different parts (leaves, flowers, twigs, roots, stem bark, immature pods, and root bark) of *S. didymobotrya* elicited antipyretic activity [27], hypolipidemic activity [28], antimicrobial activity against bacteria (such as *Bacillus cereus*, *Bacillus subtilis*, *Escherichia coli*, *Enterobacter aerogenes*, *Lactobacillus acidophilus*, *Klebsiella pneumoniae*, *Proteus vulgaris*, *Ralstonia solanacearum, Salmonella typhi*, *Serratia liquefaciens*, and *Streptococcus mitis*) [29–40] and fungi (such as *Aspergillus niger*, *Candida albicans*, *Candida glabrata*, *Candida krusei*, *Candida parapsilosis*, *Candida tropicalis*, *Candida duobushaemulonii*, *Candida haemulonii*, *Candida auris*, *Candida famata*, *Candida orientalis, Cryptococcus neoformans*, *Trichophyton mentagrophyte*, and *Microsporum gypseum*) [15, 34, 35, 40–42]. Insecticidal activity (against fleas and *Acanthoscelides obtectus*) and anthelmintic and antiamoebic activities as well as toxicity of the extracts have also been reported [34–36, 43, 44].

Classical phytochemical screening of various extracts of *S. didymobotrya* has indicated that anthraquinones, tannins, saponins, naphthoquinones, terpenes, steroids, alkaloids, flavonoids, phenols, and terpenoids are the major secondary therapeutic secondary metabolites [14, 30, 34, 36, 45, 46]. Alemayehu et al. [45] isolated and characterized for the first time 2,6,4′-trihydroxy-trans-stilbene (a stilbenoid derivative) and 4-(2′-oxymethylene-4′-hydroxyphenyl) chrysophanol (a phenyl anthraquinone) from chloroform/methanol extract of *S. didymobotrya* roots. Later, chromatographic separation of the hexane and dichloromethane extracts of *S. didymobotrya* roots led to the identification of terpenoids (3β-sitosterol and stigmasterol) and anthraquinones (chrysophanol and physcion) [35]. Recently, terpinolene and alpha-pinene were reported as the main antipyretic compounds in dichloromethane extract of *S. didymobotrya* leaves [27].

Though some pharmacological activities and toxicity of different extracts of *S. didymobotrya* parts have been reported, there is no report on the synthesis of CuNPs and antimicrobial activity of nanoparticles synthesized from this plant. The current study therefore for the first time investigated the synthesis of CuNPs using *S. didymobotrya* roots extracts and their antimicrobial efficacy against *E. coli* and *Staphylococcus aureus.* Since the synthesis of nanoparticles of smaller and uniformly distributed size, crystalline, and good stability requires control of experimental conditions [47, 48], synthesis conditions (concentration of copper ions, temperature, and pH) for the CuNPs were optimized.

2. Materials and Methods

2.1. Chemicals and Reagents. Copper (II) sulphate pentahydrate ($CuSO_4{\cdot}5H_2O$), anhydrous sodium sulphate, silica gel, and methanol were purchased from Merck Ltd., USA. All the chemicals and reagents were of analytical grade and were used without further purification. *E. coli* (ATCC 25922), *S. aureus* (ATCC 25923), Kirby–Bauer disks, amoxicillin clavulanate, and 0.5 McFarland standards were obtained from Cypress Diagnostics, Belgium.

2.2. Sample Collection and Preparation. S. didymobotrya roots were harvested from plants growing in their natural habitat in West Uyoma sublocation, Siaya County, Kenya (0°15′8S 34°16′02.8E). They were identified and authenticated at the Department of Biological Sciences, Moi University (Kenya), where a voucher specimen (SD 2018/03) was deposited for future reference.

The collected roots were washed several times with distilled water to remove dust. They were dried at room temperature under shade for three weeks. After, they were chopped into small pieces and pulverized using a laboratory mill. The extraction was carried out according to the method described by Kigondu et al. [49] with slight modifications. Weighed 50 g of the root powder was transferred into the Soxhlet apparatus and extracted with 250 mL of methanol for 48 hours. Methanol was used as the solvent of extraction because it was the best solvent of extraction according to trial extractions done using diethyl ether, methanol, and distilled water. The crude extract was concentrated by rotary evaporation at 40°C and transferred to a desiccator containing anhydrous sodium sulphate. The percentage yield of the crude extract was determined as per the following equation [50]:

$$\text{extractive yield value} = \frac{\text{weight of concentrated extract}}{\text{weight of plant dried powder}} \times 100. \quad (1)$$

2.3. Gas Chromatography-Mass Spectrometry Analyses. GC-MS analysis was performed using an Agilent 8890A GC system interfaced with a 5977B mass spectrometer detector fused with a capillary column (30×0.25 mm, $0.25\,\mu$m). For GC-MS detection, an electron ionization system was operated in electron impact mode with an ionization energy of 70 eV. Helium gas (99.999%) was used as a carrier gas at a constant flow mode of 1.2 ml/min, and an injection volume of 2 μL was employed (a split ratio of 10:1). The injector temperature was maintained at 250°C; the ion-source temperature was 200°C; and the oven temperature was programmed from 60°C (for 1.5 min), with an increase of 20°C/min to 220°C, then 5°C/min to 280°C (4 min), and ending with a 10 min isothermal at 280°C. Mass spectra were taken at 70 eV. The Jet-Clean Ion Source temperature was at 320°C, and MS Quadrupole was at 180°C with a scan interval of 0.5 s. The solvent delay was 0 to 3 min, and the total GC-MS running time was 36 min. Identification of the peaks was based on computer matching of the mass spectra with the National Institute of Standards and Technology (NIST 08) library; direct comparison with the published data was also utilized.

2.4. Synthesis, Optimization, and Characterization of CuNPs from S. didymobotrya Root Extracts

2.4.1. Synthesis of CuNPs. Synthesis of CuNPs was carried out by adding 10 mL of *S. didymobotrya* root extracts to 90 mL of 0.0125, 0.03125, and 0.05 M of $CuSO_4{\cdot}5H_2O$ solution. The reaction mixture was kept on a magnetic stirrer at 200 rpm and varying temperatures (40, 60, and 80°C) and pH (3, 6.5, and 10 pH). The reaction mixture was centrifuged at 5,000 rpm for 5 min to remove any free biomass residue. The supernatant was again centrifuged at 12,000 rpm for 40 min to obtain pellets. The pellets of CuNPs were resuspended using distilled water. The reduction of Cu ions was measured by UV-Vis spectrophotometer (Beckham Coulter DU 720, Beckham Coulter Inc., USA) after 4 hours.

2.4.2. Optimization of Synthesis of CuNPs. A three-level Box–Behnken experimental design was used for the optimization of analytical parameters affecting the synthesis of CuNPs [51] using the methanolic root extract of *S. didymobotrya.* Minitab statistical software (v17, Minitab Inc., USA) was used for the experimental design. The selected design matrix from Box–Behnken consisted of 15 trials. The parameters optimized were concentration of copper ions (0.0125–0.05 M), pH of the mixture (3.0–10.0), and temperature of the mixture (40°C–80°C) on the particle size of CuNPs. Response variables as a function of the synthesized parameters followed a second-order polynomial as follows:

$$\begin{aligned}\text{average size} = {} & -85.2 + 2.570\,\text{Temp} - 174\,\text{Conc} + 16.97\,\text{pH} - 0.02691\,\text{Temp} * \text{Temp} \\ & - 5813\,\text{Conc} * \text{Conc} - 0.9391\,\text{pH} * \text{pH} + 8.41\,\text{Temp} * \text{Conc} + 0.0278\,\text{Temp} - 23.1\,\text{Conc} * \text{pH}.\end{aligned} \quad (2)$$

where Conc = concentration and Temp = temperature.

2.4.3. Ultraviolet-Visible Spectroscopy. Synthesized CuNPs (300 μL) were diluted with 3 mL of distilled water and scanned on a UV-Vis spectrophotometer (Beckham Coulter DU 720, Beckham Coulter Inc., USA) from 300 to 700 nm at a resolution of 1 nm using distilled water as the blank [52].

2.4.4. Particle Size Analysis. The sizes of synthesized CuNPs were measured using a particle size analyzer (Microtrac Nanotrac Wave II, SL-PS-25 Rev. H) with a laser diode detector.

2.4.5. X-Ray Diffraction Analysis. The synthesized CuNPs were subjected to an X-ray diffraction (XRD) analyzer operated at the voltage of 40 kV and 20 mA with copper $K\alpha$ radiation in the range of θ–2θ configuration with a scanning rate of 0.030°C/s. The crystallite size (CS) was calculated using Debye–Scherrer equation as follows [52, 53]:

$$\text{CS} = \frac{K\lambda}{\cos\,\theta}, \quad (3)$$

where constant $(K) = 0.94$, $\lambda = 1.5406 \times 10^{-10}$, $\cos\,\theta$ = Bragg angle, and β is the full width at half maximum (FWHM). Full width at half maximum in radius (β) = FWHM $\times\, \pi/180$.

2.4.6. FT-IR Analysis. FT-IR analysis was performed to identify functional groups bound on the surface of the CuNPs. The specimen and potassium bromide granules were powdered together in a ratio of 1:100 (w/w) and then compressed into pellets. Subsequently, the analysis was performed and measured using FT-IR spectrophotometer in the range of 400–4,000 cm^{-1} and with a resolution of 4 cm^{-1} [52, 53].

2.5. Antibacterial Activity of the Synthesized CuNPs from the S. didymobotrya Root Extract. The antimicrobial efficacy of biosynthesized 4 cm^{-1} CuNPs was assessed using Kirby–Bauer disk diffusion susceptibility test protocol [54]. The test microorganisms were chosen according to the National

Committee for Clinical Laboratory Standards 2010 protocols [55]. Gram-negative *E. coli* and Gram-positive *S. aureus* were tested. Amoxicillin clavulanate impregnated antimicrobial susceptibility testing discs were used as a positive control. All bioassay was done with 30 μL of solution of CuNPs resuspended in distilled water, *S. didymobotrya* root extract, and copper sulphate solution as per the specification of the positive control (amoxicillin clavulanate). After 18 hours of incubation, the zone of inhibition diameter (ZOI) was measured to the nearest millimetre using a ruler and recorded. The susceptibility or resistance of the test organism to each drug tested was determined using the published Clinical Laboratory Standards Institute (CLSI). The ZOI was classified as susceptible (*S*), intermediate (*I*), or resistant (*R*) based on the CLSI interpretive criteria [50].

3. Results and Discussion

The percentage yield of *S. didymobotrya* root powder was 9.94% as calculated using equation (1).

3.1. GC-MS Results. The GC-MS analysis on *S. didymobotrya* methanolic root extract was conducted to identify the active phytochemicals that might take part in the fabrication of CuNPs. The results indicated that the extract contained mainly fatty acids and some volatile organic compounds. The compounds along with their retention times, abundances, molecular formulae, and molecular weights are presented in Table 1. The major compounds identified were benzoic acid, thymol, *n*-benzyl-2-phenethylamine, benzaldehyde, vanillin, phenylacetic acid, and benzothiazole.

There is a paucity of literature on volatile compounds in *S. didymobotrya*. This study presented the first comprehensive report on the GC-MS analysis of volatile compounds in *S. didymobotrya* extract. Previously, Mworia et al. [27] reported the presence of terpinolene and alpha-pinene as the main antipyretic compounds in dichloromethane extract of *S. didymobotrya* leaves using GC-MS. None of the foregoing compounds were identified in this study. Interestingly, some compounds identified in the methanolic extract of *S. didymobotrya* roots in this study have a potential to take part in the formation of nanoparticles. For instance, alizarin (a dihydroxyanthraquinone with two hydroxyl groups on a phenyl ring) possesses a structure similar to compounds proposed to take part in chelation and reduction of copper ions to CuNPs [2, 56].

3.2. Synthesis and Characterization of CuNPs. Bioreduction of copper ions to CuNPs on exposure to methanolic extract of *S. didymobotrya* roots was monitored by observing the colour change and using UV–visible spectroscopy. There was a gradual colour change from light orange solution to dark brown, indicating the formation of CuNPs after 4 hours [57–61]. Pretrial runs indicated that no significant changes occurred after 3 hours. Usually, small metal nanoparticles absorb visible electromagnetic waves through the collective oscillation of conduction electrons at the surface, a phenomenon known as surface plasmon resonance (SPR) effect [62]. Thus, the final dark colour observed could be ascribed to the excitation of surface plasmon vibrations, indicating the formation of CuNPs [10, 52]. Copper oxides are thermodynamically more stable than copper sulphates, which leads to the aggregation and oxidation of copper without proper protection [62]. Thus, the addition of the *S. didymobotrya* root extract might have inhibited the oxidation of copper, thereby acting as a reducing and capping agent for the CuNPs [10].

The UV–Visible spectrum of the methanolic root extract of *S. didymobotrya* (Figure 1(a)) showed bands at λ_{max} 338 nm (band II). The band at 338 nm (band II) can either be due to $n \longrightarrow \pi*$ transition or a combination of $n \longrightarrow \pi*$ and $\pi \longrightarrow \pi*$ transitions of heteroatoms linked in a double bond. The presence of quercetin, a class of flavonoids, has also been reported as a major constituent of the crude aqueous root extract of *S. didymobotrya* [63]. The observed transitions are probably related to quercetin involved in the reduction process and formation of CuNPs via π-electron interactions [56, 64]. Hence, the extract of *S. didymobotrya* roots further acted as a reductant and stabilizer agent.

The UV–Vis spectrum of the CuNPs (Figure 1(b)) showed changes in the absorbance maxima due to surface SPR, demonstrating the formation of CuNPs [65, 66]. The SPR peak, which is a signature of the formation of CuNPs, appears in the visible region [67, 68] at 542, 570, 604, 616, 638, 662, and 694, nm with absorbances of 0.064, 0.153, 0.066, 0.064, 0.065, 0.072, and 0.970, respectively (Figure 1). According to Mei's theory, the occurrence of a single UV-visible peak in the UV-Visible spectrum of synthesized nanoparticles confirms that they are spherical in shape [58].

3.3. Design of Experiments and Optimization Analysis. Table 2 contains the list of experimental runs and the corresponding responses obtained from the experiments projected by Box–Behnken design. The design optimized parameters that would yield CuNPs with the least average particle size. The experiments were done as per the run order to eliminate experimental bias. The mean particle size of CuNPs was recorded on particle size analyzer (Nanotrac).

A regression coefficient (R^2) of 0.9964 was obtained with a second-order quadratic equation generated for the optimization process. The adequacy of the model was checked using ANOVA. The predictor variables, that is, pH, concentration of copper ions, and temperature, of the mixture were all significant [47]. The value of $p \leq 0.05$ indicated that pH ($p \leq 0.001$) is the most influencing factor when compared to the concentration of copper ion ($p \leq 0.003$) and temperature of the mixture ($p \leq 0.001$). Variance inflation factors (VIF) value close to 1 indicates that the predictors are not correlated (Table 3) [69]. The qualities of the fitted models were evaluated based on the coefficients of determination (R^2) that was 0.9964. The model explains 99.64% of the variation in the average size data. The adjusted R^2 is 99.00%. R^2 (pred) is 94.31%, which indicates that the model explains 94.31% of the variation in the average size of CuNPs when used for prediction.

Table 1: Compounds identified by GC-MS in *S. didymobotrya* methanolic root extract.

SN	Retention time (mins)	Compound	Molecular formula	Molecular weight (g/mol)
1	14.4375	Benzoic acid	$C_7H_6O_2$	122.12
2	12.4726	Benzyl alcohol	C_7H_8O	108.14
3	16.7112	Thymol	$C_{10}H_{14}O$	150.22
4	11.0757	N-Benzyl-2-phenethylamine	$C_{15}H_{17}N$	211.3022
5	17.5703	Benzaldehyde	C_7H_6O	106.1219
6	18.3040	Vanillin	$C_8H_8O_3$	152.15
7	15.7370	Phenylacetic acid	$C_8H_8O_2$	136.15
8	15.9515	Nonanoic acid	$C_9H_{18}O_2$	158.24
9	16.0344	Benzothiazole	C_7H_5NS	135.19
10	14.3651	Tuaminoheptane	$C_7H_{17}N$	115.2166
11	11.5752	Furfurylmethylamphetamine	$C_{15}H_{19}NO$	229.3175
12	17.8169	Disiloxane	H_6OSi_2	78.22
13	18.6719	Barbital/barbitone	$C_8H_{12}N_2O_3$	184.195
14	30.7212	6H-Dibenzo (b,d) pyran-1-ol,6a-beta,7,8,10-a-beta-tetrahydro-3-pentyl-6,6,9-trimethyl-,(+-)-Z-	$C_{21}H_{30}O_2$	314.5
15	33.5783	Oxymetazoline	$C_{16}H_{24}N_2O$	260.381
16	21.5570	1-Methyl-9H-pyrido (3,4-b) indole	$C_{12}H_{10}N_2$	182.2212
17	10.7265	3-Carene	$C_{10}H_{16}$	136.2340
18	19.1589	5-Hexyldihydro-2(3H)-furanone	$C_{10}H_{18}O_2$	170.2487
19	19.1900	2,6-bis-(1,1-Dimethylethyl)-2,5-cyclohexadien-1,4-dione	$C_{14}H_{20}O_2$	220.3074
20		9,12-Hexadecadienoic acid, methyl esther	$C_{19}H_{34}O_2$	294.4721
21	12.0521	3-Amino-s-triazole	$C_2H_4N_4$	84.0800
22	18.4926	Diphenylether	$C_{12}H_{10}O$	170.2072
23	7.4527	Formamide	CH_3NO	45.0406
24	14.7857	Glycine	$C_2H_5NO_2$	75.0666
25	17.205	Thiocyanic acid, 4-(dimethylamino) phenyl ester	$C_9H_{10}N_2S$	178.26
26	9.4063	2-(p-Tolyl) ethylamine	$C_9H_{13}N$	
27	4.3626	Methyl vinylketone	C_4H_6O	70.0898
28	28.5117	Pyrene	$C_{16}H_{10}$	202.2506
29	22.3363	4H-1-Benzopyran-4-one	$C_9H_6O_2$	146.1427
30	16.8355	Methane, isocyanato-/isocyanic acid/methyl isocyanate	C_2H_3NO	57.0513
31	23.6700	Phenanthrene	$C_{14}H_{10}$	178.2292
32	26.7448	Menthol	$C_{10}H_{20}O$	156.269
33	32.1937	Alizarin	$C_{14}H_8O_4$	240.21
34	14.7857	N-Benzylglycine	$C_9H_9NO_3$	169.19
35	13.0157	4-(2-Aminoethyl) phenol	$C_8H_{13}NO_2$	155.19
36	14.6250	Benzeneethanamine, N,alpha-dimethyl-N-(phenylmethyl)-, hydrochloride	$C_{17}H_{22}ClN$	275.82
37	14.7857	Acetophenone	C_8H_8O	120.15
38	21.5570	2,4,6-Trimethoxyamphetamine	$C_{12}H_{19}NO_3.HCl$	261.70
39	32.8342	(2-Chlorophenyl)-bis[4-(dimethylamino)phenyl]methanol	$C_{23}H_{25}ClN_2O$	380.9
40	7.4527	Formamide	CH_3NO	45.04
41	8.2517	Aniline	C_6H_7N	93.13
42	8.6932	4-Methyl-4-hydroxy-2-pentanone	$C_6H_{12}O_2$	116.1583
43	10.1989	Hexylene glycol	$C_6H_{14}O_2$	118.17
44	11.0757	Propylbenzene	C9H12	120.2
45	11.6747	2-(2-Ethoxyethoxy)ethanol	$C_6H_{14}O_3$	134.17
46	11.8208	1,3,5-Trimethylbenzene	C_9H_{12}	164.7
47	12.1959	2-Ethylhexan-1-ol	$C_8H_{18}O$	130.2279
48	12.2944	1,3-Dichlorobenzene	$C_6H_4Cl_2$	147.002
49	14.0562	1,2,3,5-Tetramethylbenzene	$C_{10}H_{14}$	134.22
50	14.1173	2-Hydroxy-3,5,5-trimethyl-2-cyclohexen-1-one	$C_9H_{14}O_2$	154.21
51	22.0834	Methyl tetradecanoate	$C_{15}H_{30}O_2$	242.2
52	22.3954	1-(4-Hydroxy-3,5-dimethoxyphenyl)ethanone	$C_{10}H_{12}O_4$	196.1999
53	23.7934	1,2-Benzenedicarboxylic acid, bis(2-methylpropyl) ester	$C_{16}H_{24}O_4$	278.3435
54	15.1598	4-Tert-butylphenol	$C_{10}H_{14}O$	150.22

Figure 2 presents the main effects plot for the average size of CuNPs. The temperature of the reaction mixture, the concentration of copper ion, and pH of the medium affect the average size of CuNPs. Comparing the slopes of the lines, it can be concluded that pH had the greater magnitude of effects.

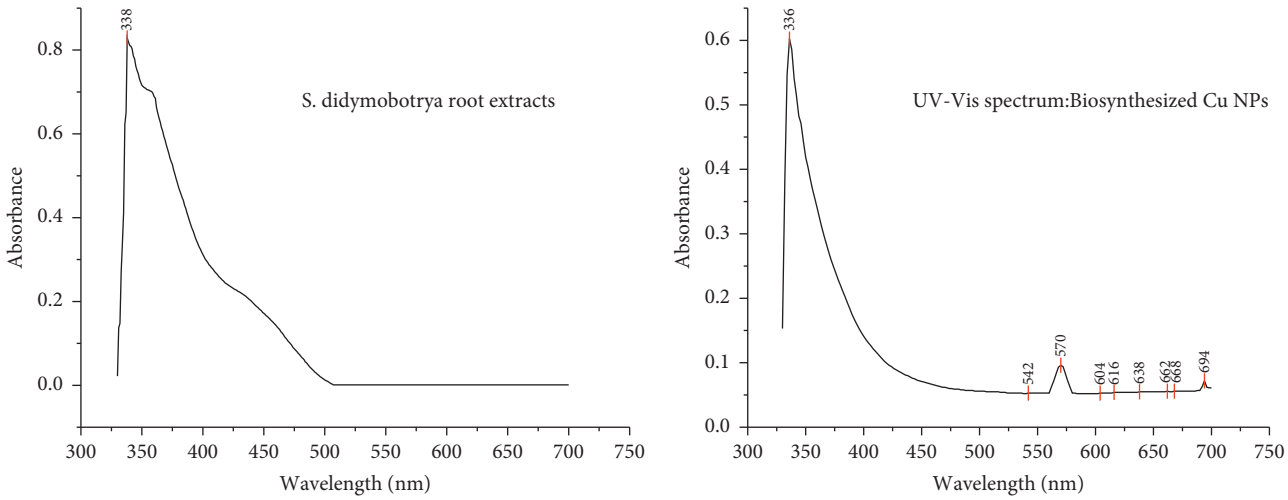

Figure 1: UV-visible spectra of (a) *S. didymobotrya* methanolic root extract and (b) CuNPs synthesized from *S. didymobotrya* methanolic root extract.

Table 2: Box–Behnken design and response variables.

Std order	Run order	PtType	Blocks	Temp (°C)	Conc (M)	pH	Size (nm)
15	1	0	1	60	0.03125	6.5	53.59
1	2	2	1	40	0.0125	6.5	53.5
9	3	2	1	60	0.0125	3	21.63
5	4	2	1	40	0.03125	3	16.11
11	5	2	1	60	0.0125	10	63.6
14	6	0	1	60	0.03125	6.5	53.58
3	7	2	1	40	0.05	6.5	38.65
2	8	2	1	80	0.0125	6.5	36.59
8	9	2	1	80	0.03125	10	50.41
4	10	2	1	80	0.05	6.5	34.35
10	11	2	1	60	0.05	3	19.5
13	12	0	1	60	0.03125	6.5	53.57
12	13	2	1	60	0.05	10	55.4
6	14	2	1	80	0.03125	3	5.55
7	15	2	1	40	0.03125	10	53.18

Table 3: Calculated values of the coefficients of the model.

Term	Effect	Coeff	SE coeff	*T*-value	*p* value	VIF
Constant		53.580	1.020	52.65	0.001	
Temp	−8.635	−4.317	0.623	−6.93	0.001	1.00
Conc	−6.855	−3.427	0.623	−5.50	0.003	1.00
pH	39.950	19.975	0.623	32.05	0.001	1.00
Temp ∗ Temp	−21.528	−10.764	0.917	−11.73	0.001	1.01
Conc ∗ Conc	−4.088	−2.044	0.917	−2.23	0.076	1.01
pH ∗ pH	23.008	−11.504	0.917	−12.54	0.001	1.01
Temp ∗ Conc	6.305	3.153	0.881	3.58	0.016	1.00
Temp ∗ pH	3.895	1.948	0.881	2.21	0.078	1.00
Conc ∗ pH	−3.035	−1.518	0.881	−1.72	0.146	1.00

Conc = concentration and Temp = temperature.

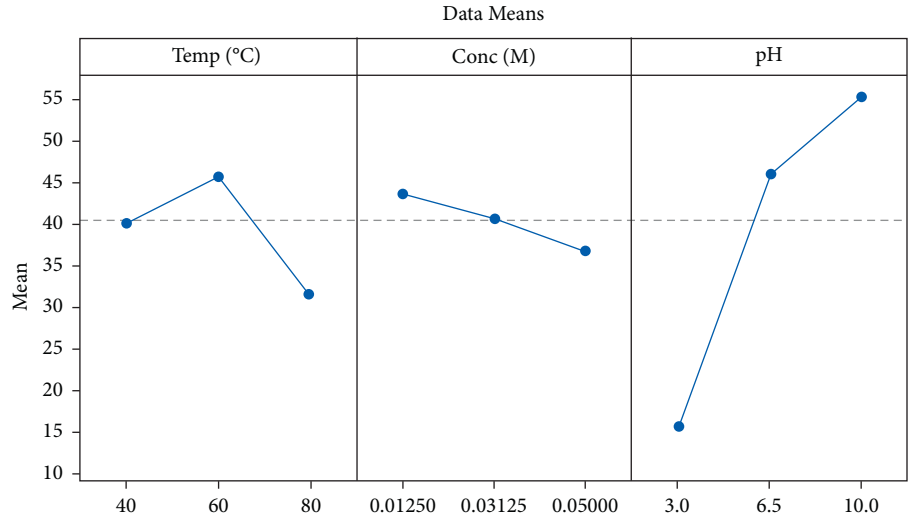

Figure 2: Main effects plot for the average size of Cu NPs.

Figure 3 presents an interaction effects plot for mean size for Cu NPs. From the plot, it is seen that there was the interaction of temperature and concentration and the interaction of concentration and pH as shown by lines intersecting at a point, but there was no possible interaction of temperature and pH as indicated by lines being approximately parallel from each other.

3.3.1. Effect of pH. The pH of range 3–10 was varied during CuNPs average size optimization process. The study revealed that pH as a parameter strongly influenced the size of CuNPs as shown by Figure 3 of the interaction effects plot for mean particle size. The least average size of the nanoparticles was recorded at a lower pH of 3.0. It was observed that increasing the pH increased the mean size of the nanoparticles. Similar observations have been reported by Honary et al. [70] and Dang et al. [62]. A possible explanation for this observation is that at a pH of 3.0, nanoparticles were experiencing high electrostatic repulsion, hence reducing agglomeration. Therefore, at alkaline pH, the nanoparticles were exhibiting lower electrostatic forces hence allowing particle growth.

3.3.2. Effect of Copper Ion Concentration. Copper ion concentration (0.0125–0.05 M) was varied for CuNPs average size optimization. The least mean size of nanoparticles was recorded at lower concentrations of copper salt as revealed in Figure 3. This finding agrees with previous findings [70, 71] that reported that high salt ion concentrations led to large particle sizes and broad size distribution of synthesized nanoparticles. This could be because a low concentration of salt reduced the probability of copper-copper interactions, hence reducing agglomeration.

3.3.3. Effect of Temperature. A temperature of range 40–80°C was controlled for CuNPs mean size optimization. The study showed that an increase in temperature from 40–80°C led to a reduction in the mean size of CuNPs. A previous research has reported similar findings [71]. This could be due to possible agglomeration at lower temperatures. (Figure 4).

According to Figure 5, the predicted average particle size is 1.7862 nm. Increasing temperature yields small particle size nanoparticles. Decrease in salt concentration and pH favours synthesis of CuNPs of the least mean size. These observations agree with those of Dang et al. [62]. Previous studies [72, 73] indicated that the pH of aqueous media influences copper reduction reaction in CuNPs synthesis. Probable kinetic enhancement is thus conducive for the reduction of crystallite size because of the enhancement of the nucleation rate [62].

3.4. Characterization Results for the CuNPs

3.4.1. Particle Size Analysis. Particle size analysis was conducted for thirteen (13) samples of CuNPs prepared at varied conditions of pH of the reaction medium, copper ion concentration, and temperature of the solution. The smallest particle was for CuNPs prepared at 80°C, pH 3.0, and copper ion concentration of 0.03125 M (Figure 6).

3.4.2. X-Ray Diffraction Results. The XRD peaks were assigned in comparison with the standard powder diffraction card of the Joint Committee on Powder Diffraction Standards (JCPDS card no. 89-2838). The peak positions were consistent with metallic copper of a crystalline nature. X-ray diffraction spectrum (Figure 7) revealed diffraction peaks at 2θ values of 43.30°, 50.02°, and 73.41° corresponding to the Miller indices (111), (200), and (220), respectively, which represent face-centred cubic structure of copper [66]. Further, the peak at 30.0° showed that a small amount of copper is oxidized to copper (II) oxide. The average size of CuNPs as determined using Debye–Scherrer's formula was 6 nm, which is close to 5.55 nm as established by XRD analysis. The size of the crystal under 100 nm suggested that the nanocrystalline nature of the biosynthesized CuNPs was

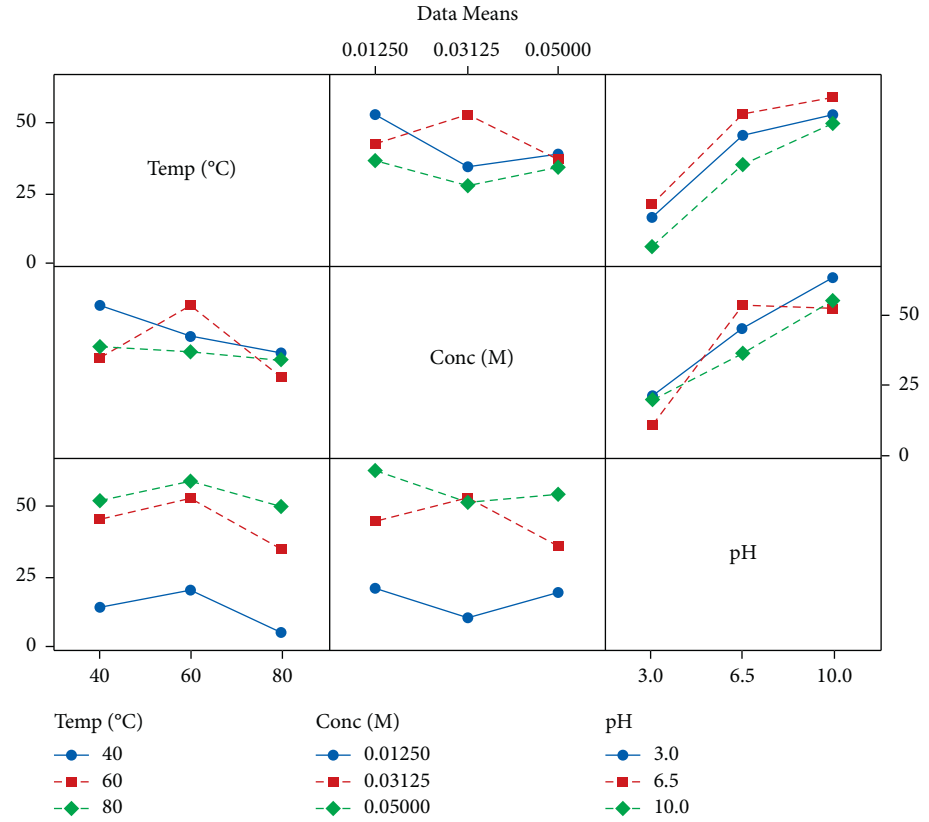

Figure 3: Interaction effects plot for mean particle size of CuNPs synthesized using *S. didymobotrya* root extract.

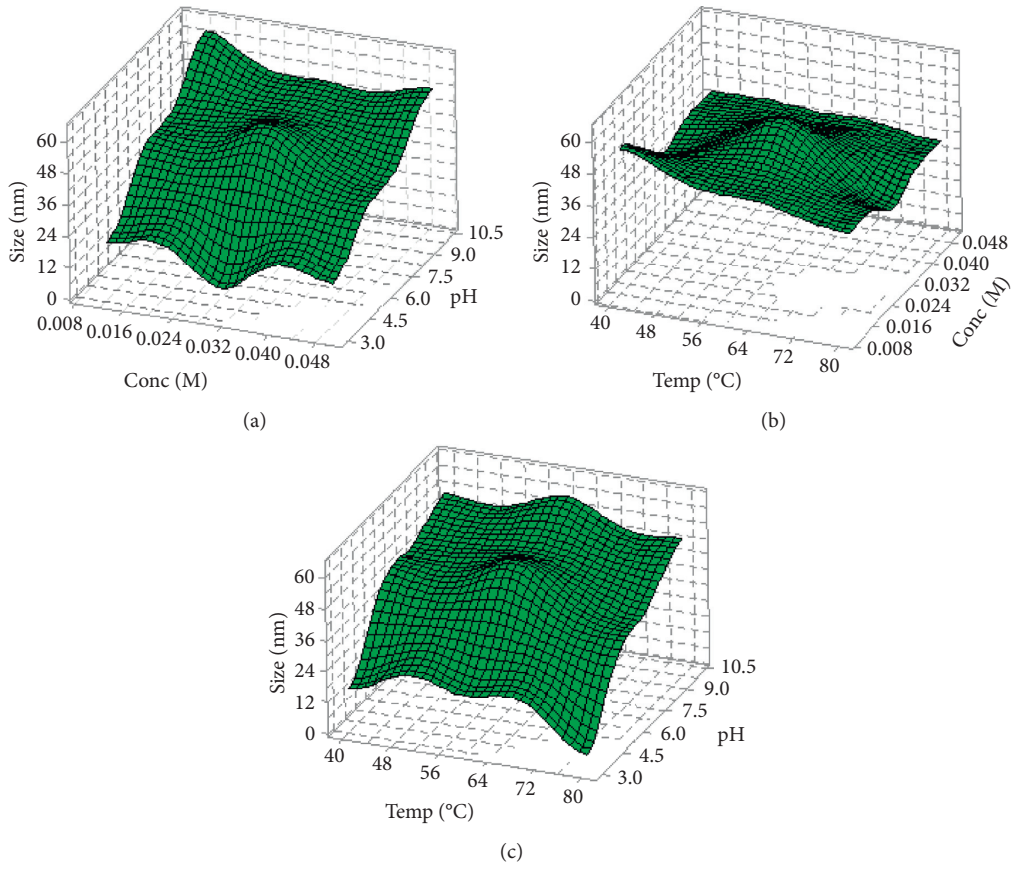

Figure 4: 3 D response surface curves: (a) mean particle size versus concentration and pH, (b) mean particle size versus temperature and concentration, and (c) mean particle size versus temperature and pH.

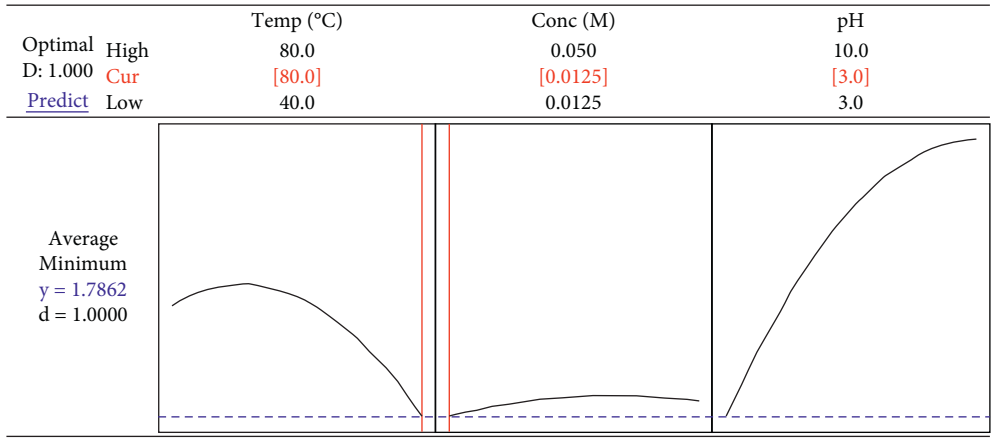

Figure 5: Response optimization for average particle size of CuNPs from *S. didymobotrya* root extract.

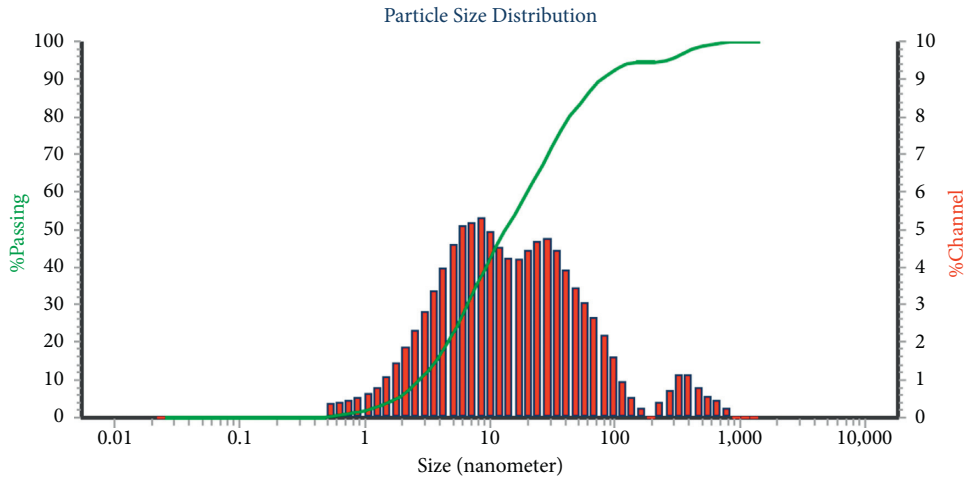

Figure 6: Particle size of CuNPs prepared at 80°C, pH 3.0, and copper ion concentration of 0.03125 M.

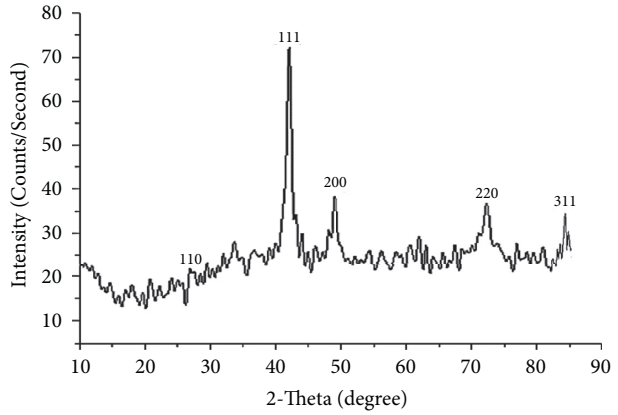

Figure 7: X-ray diffraction pattern of CuNPs synthesized from *S. didymobotrya* root extract.

below 15 nm [57]. Similar results were reported by other researchers from the structure analysis of XRD for biosynthesized CuNPs [57, 58, 60].

3.4.3. Zeta Potential of the CuNPs. The zeta potential value of biosynthesized CuNPs was −69.4 mV (Figure 8). This indicated that the biosynthesized CuNPs surfaces possessed

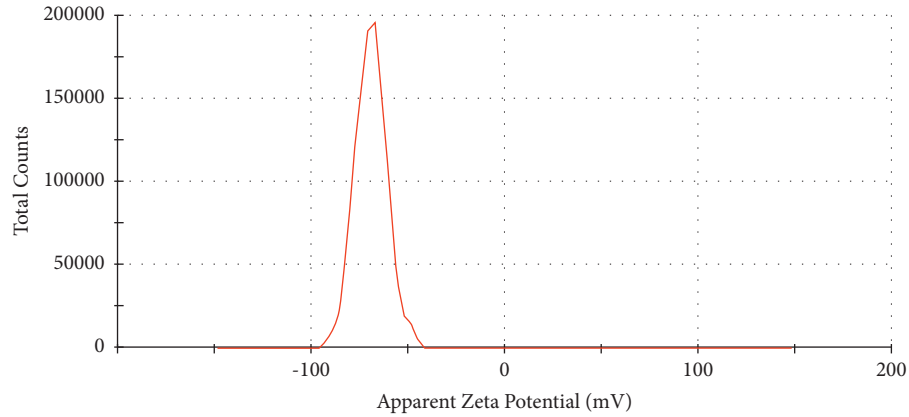

Figure 8: Zeta potential distribution of CuNPs synthesized using *S. didymobotrya* root extract.

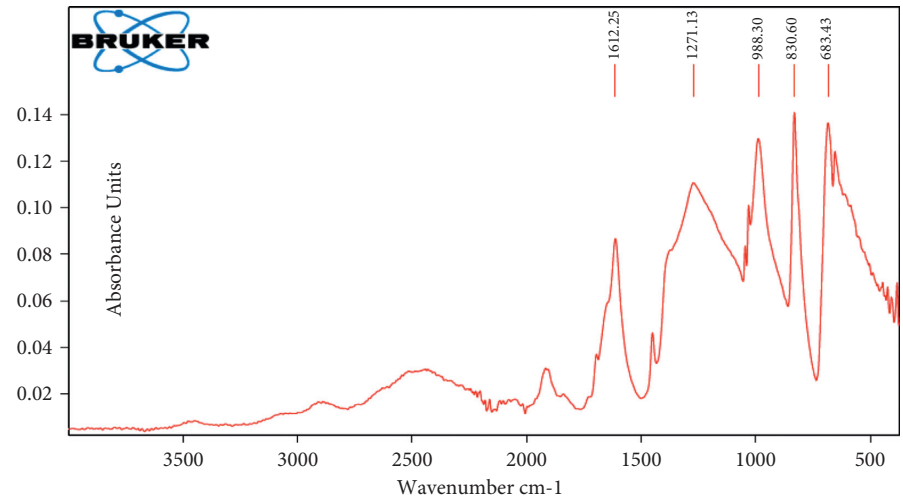

Figure 9: FT-IR spectrum of CuNPs synthesized from *S. didymobotrya* root extract.

strong electrostatic repulsion hence good stability. A recent study [61] indicated that CuNPs of size 82.32 nm had a negative zeta potential of −11.9 mV. Such negative zeta potentials suggest that charge distribution of the nanoparticles as well as their sizes could play a role in promoting or enhancing their biological properties [74]. In other words, high negative zeta potential translates into strong repulsion between the particles causing amplification or enhancement of their stabilities [75].

3.4.4. FT-IR Analysis. FT-IR analysis was done to identify the functional groups of the phytochemicals that participated in synthesizing CuNPs and their stabilization. The spectrum shown in Figure 9 revealed a broadband in the range 3,400–3,500 cm^{-1} characteristic of N-H stretch of amines and amides, and a band of the range 3400–2400 cm^{-1} indicating the presence of O-H of carboxylic acids, alcohols, and phenols. The peak at 1,612.25 cm^{-1} is assigned to C=C of alkenes and aromatic compounds. The presence of aromatic compounds was confirmed by the two peaks at 988.30 cm^{-1} and 830.60 cm^{-1} known for C-H out-of-plane bend for aromatic compounds. A peak at 1,271.13 cm^{-1} is attributed to C-O bond of alcohols, carboxylic acids, and esters.

The presence of these functional groups indicated the possible involvement of reductive groups on the surfaces of the CuNPs [76]. They are also involved in the capping of the CuNPs, as observed in previous studies that synthesized CuNPs from plant extracts [10, 77]. The spectrum indicated new chemical linkages on the surface of CuNPs, suggesting that *S. didymobotrya* root extract can bind to CuNPs through hydroxyl and carbonyl groups of the amino acid residues in the protein of the extracts, therefore acting as reducing, stabilizing, and dispersing agents for synthesized copper oxide nanoparticles and preventing agglomeration of the CuNPs [60, 61].

3.5. Antibacterial Activity of S. didymobotrya Root Extract and Synthesized CuNPs. Figure 10 shows that the CuNPs had an inhibitory effect against *E. coli* and *S. aureus*. Pearson's product-moment correlation was performed to evaluate the association between the size of CuNPs and ZOI of CuNPs against *E. coli* and *S. aureus* ($n = 13$). The analysis showed that there was a negative correlation between the size of CuNPs and the zone of inhibition of *E. coli* ($r = -0.74$; $p \geq 0.01$). Similarly, a negative correlation was observed between the size of CuNPs and the zone of inhibition of *S. aureus* by the CuNPs ($r = 0.74$; $p \geq 0.05$).

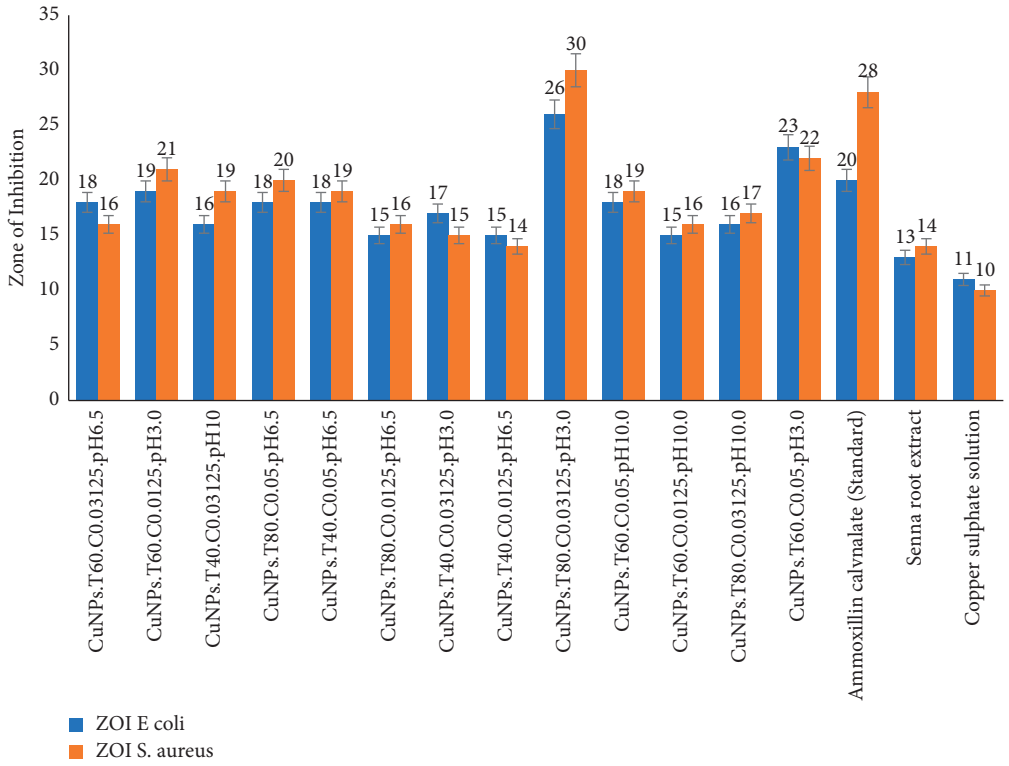

Figure 10: Antibacterial activity of CuNPs, amoxicillin clavulanate, copper sulphate solution, and *S. didymobotrya* methanolic root extract.

The highest zone of inhibition was 30.00 ± 0.58 mm for *S. aureus* and 26.00 ± 0.58 mm for *E. coli* was achieved for CuNPs with the least mean particle size that was synthesized at optimum conditions of 80°C, copper ion concentration of 0.03125 M, and pH 3.0. This indicated that CuNPs of least mean particle size had a high surface area to volume ratio, hence effectively binding to the microbial membrane and probably altered its permeability that could have caused growth inhibition. Sathiyavimal et al. [10] reported similar results in which 100 μL of CuNPs prepared from *Sida acuta* extract highly inhibited *E. coli* with a zone of inhibition maximum of 15 mm, showed a lower antibacterial activity against *S. aureus* while the lowest inhibition diameter was 11 mm against *P. vulgaris*. Previous authors [66, 78, 79] have reported similar results, in which *E. coli* was the most inhibited bacteria when compared with *S. aureus* and other Gram-positive bacteria.

The higher inhibition of Gram-negative bacteria by CuNPs could be partially explained by the facilitated influx of smaller-sized nanoparticles into the cell wall of Gram-negative bacteria that consists of a unique outer membrane layer and a single peptidoglycan layer as compared to the cell wall of Gram-positive bacteria with several peptidoglycan layers [80, 81]. Furthermore, CuNPs have been speculated to adhere to Gram-negative bacterial cell walls due to electrostatic interaction, or the copper ions facilitate rapid DNA degradation and reduction of bacterial respiration [82]. In some Gram-negative strains, copper ions alter the conformation and electron transferase of the associated reductases, culminating in the inhibition of cytochromes in the membrane [83].

4. Conclusion

Synthesis of CuNPs from *S. didymobotrya* methanolic root extract had the following optimum synthesis conditions: temperature 80°C, pH 3.0, and copper ion concentration of 0.0125 M. The mean particle size of CuNPs predicted by the design at the optimum conditions was 1.7862 nm. UV-Vis analysis showed a characteristic surface plasmon resonance peak at 571 nm indicating the formation of CuNPs. FT-IR analysis revealed that the nanoparticles were bound by carboxylic acids, amines, and amides, phenols, and esters. Particle size analysis conducted using Nanotrac particle analyzer showed that synthesized CuNPs were of the range of 5.55–63.60 nm particle size. X-ray diffraction measurement confirmed the presence of cubic face centred CuNPs. The measured zeta potential value of CuNPs was −69.4 mV indicating that they were stable. In conclusion, the biosynthesized Cu nanoparticles are stable and displayed better antimicrobial activity against *E. coli* and *S. aureus* compared to amoxicillin clavulanate (standard). The study recommends the testing of biosynthesized CuNPs against other potential multidrug resistant microbes to enable their development into antimicrobial agents.

Abbreviations

CuNPs: Copper nanoparticles
E. coli: *Escherichia coli*
S. didymobotrya: *Senna didymobotrya*
SPR: *Surface* plasmon resonance.

Data Availability

The datasets supporting the conclusions of this study are available from the corresponding author upon request.

Conflicts of Interest

The authors declare that there are no conflicts of interest regarding the publication of this paper.

Acknowledgments

The authors are grateful to the World Bank and the Inter-University Council of East Africa for the fellowship awarded to Bernard Otieno Sadia through the Africa Center of Excellence II in Phytochemicals, Textile and Renewable Energy at Moi University, Kenya. This study was financially supported by the Africa Center of Excellence II in Phytochemicals, Textile and Renewable Energy (ACE II PTRE) hosted at Moi University, Kenya (Credit No. 5798-KE). Timothy Omara (Department of Chemistry and Biochemistry, Moi University) is acknowledged for his tireless guidance in preparing and English proofreading of this article.

References

[1] G. E. Poinern, *A Laboratory Course in Nanoscience and Nanotechnology*, CRC Press, Taylor and Francis Group, Boca Raton, FL, USA, 2015.

[2] M. F. Al-Hakkani, "Biogenic copper nanoparticles and their applications: a review," *SN Applied Sciences*, vol. 2, no. 3, p. 505, 2020.

[3] P. Padma, S. Banu, and S. Kumari, "Studies on green synthesis of copper nanoparticles using *Punica granatum*," *Annual Research & Review in Biology*, vol. 23, no. 1, pp. 1–10, 2018.

[4] R. Betancourt-Galindo, P. Y. Reyes-Rodriguez, B. A. Puente-Urbina et al., "Synthesis of copper nanoparticles by thermal decomposition and their antimicrobial properties," *Journal of Nanomaterials*, vol. 2014, Article ID 980545, 5 pages, 2014.

[5] R. Kavita and K. Sharma, "Biological synthesis of copper nanoparticles and their antimicrobial properties: a review," *World Journal of Pharmaceutical Research*, vol. 7, no. 7, pp. 514–539, 2018.

[6] G. Granata, T. Yamaoka, F. Pagnanelli, and A. Fuwa, "Study of the synthesis of copper nanoparticles: the role of capping and kinetic towards control of particle size and stability," *Journal of Nanoparticle Research*, vol. 18, no. 5, p. 133, 2016.

[7] G. Caroling, M. N. Priyadharshini, E. Vinodhini, A. M. Ranjitham, and P. Shanthi, "Biosynthesis of copper nanoparticles using aqueous guava extract," *International Journal Pharmacy and BioScience*, vol. 5, pp. 25–43, 2015.

[8] O. B. Adewale, K. A. Egbeyemi, J. O. Onwuelu et al., "Biological synthesis of gold and silver nanoparticles using leaf extracts of *Crassocephalum rubens* and their comparative in vitro antioxidant activities," *Heliyon*, vol. 6, no. 11, Article ID e05501, 2020.

[9] D. N. Williams, S. H. Ehrman, and T. R. Pulliam Holoman, "Evaluation of the microbial growth response to inorganic nanoparticles," *Journal of Nanobiotechnology*, vol. 4, no. 1, p. 3, 2006.

[10] S. Sathiyavimal, S. Vasantharaj, D. Bharathi et al., "Biogenesis of copper oxide nanoparticles (CuONPs) using *Sida acuta* and their incorporation over cotton fabrics to prevent the pathogenicity of gram negative and gram positive bacteria," *Journal of Photochemistry and Photobiology B: Biology*, vol. 188, pp. 126–134, 2018.

[11] D. Vaidehi, V. Bhuvaneshwari, D. Bharathi, and B. P. Sheetal, "Antibacterial and photocatalytic activity of copper oxide nanoparticles synthesized using *Solanum lycopersicum* leaf extract," *Materials Research Express*, vol. 5, no. 8, Article ID 085403, 2018.

[12] D. Bharathi, R. Ranjithkumar, B. Chandarshekar, and V. Bhuvaneshwari, "Bio-inspired synthesis of chitosan/copper oxide nanocomposite using rutin and their anti-proliferative activity in human lung cancer cells," *International Journal of Biological Macromolecules*, vol. 141, pp. 476–483, 2019.

[13] G. Killivalavan, A. C. Prabakar, and K. Chandra Babu, "Synthesis and characterization of pure and Cu doped CeO_2 nanoparticles: photocatalytic and antibacterial activities evaluation," *Biointerface Research in Applied Chemistry*, vol. 10, no. 2, pp. 5306–5311, 2020.

[14] L. B. Nyamwamu, M. Ngeiywa, M. Mulaa, and A. E. Lelo, "Phytochemical constituents of *Senna didymobotrya* fresen irwin roots used as a traditional medicinal plant in Kenya," *International Journal of Educational Research*, vol. 2, pp. 435-436, 2015.

[15] P. Jeruto, P. F. Arama, B. Anyango et al., "In vitro antifungal activity of methanolic extracts of different *Senna didymobotrya* (fresen.) H.S. Irwin & Barneby plant parts," *African Journal of Traditional, Complementary, and Alternative Medicines*, vol. 13, no. 6, pp. 168–174, 2016.

[16] T. Omara, "Plants used in antivenom therapy in rural Kenya: ethnobotany and future perspectives," *Journal of Toxicology*, vol. 2020, Article ID 1828521, 9 pages, 2020.

[17] G. N. Njoroge and R. W. Bussmann, "Diversity and utilization of antimalarial ethnophytotherapeutic remedies among the Kikuyus (Central Kenya)," *Journal of Ethnobiology and Ethnomedicine*, vol. 2, no. 8, p. 8, 2006.

[18] N. Mukungu, K. Abuga, F. Okalebo, R. Ingwela, and J. Mwangi, "Medicinal plants used for management of malaria among the Luhya community of Kakamega East sub-County, Kenya," *Journal of Ethnopharmacology*, vol. 194, pp. 98–107, 2016.

[19] P. G. Kareru, G. M. Kenji, A. N. Gachanja, J. M. Keriko, and G. Mungai, "Traditional medicines among the Embu and Mbeere people of Kenya," *African Journal of Traditional, Complementary and Alternative Medicines*, vol. 4, pp. 75–86, 2007.

[20] S. V. Okello, R. O. Nyunja, G. W. Netondo, and J. C. Onyango, "Ethnobotanical study of medicinal plants used by Sabaots of Mt. Elgon Kenya," *African Journal of Traditional, Complementary and Alternative Medicines*, vol. 7, no. 1, pp. 1–10, 2010.

[21] C. N. Olala, "Identification of plants used for treatment of malaria and factors influencing their use in Boro division, Siaya county, Kenya," MSc thesis, Kenyatta University, Nairobi, Kenya, 2014.

[22] J. Nankaya, J. Nampushi, S. Petenya, and H. Balslev, "Ethnomedicinal plants of the loita Maasai of Kenya," *Environment, Development and Sustainability*, vol. 15, no. 5, 2019.

[23] M. Gakuubi and W. Wanzala, "A survey of plants and plant products traditionally used in livestock health management in Buuri district, Meru County, Kenya," *Journal of Ethnobiology and Ethnomedicine*, vol. 8, no. 1, p. 39, 2012.

[24] T. Omara, "Antimalarial plants used across kenyan communities," *Evidence-Based Complementary and Alternative Medicine*, vol. 2020, Article ID 4538602, 31 pages, 2020.

[25] P. Jeruto, C. Lukhoba, G. Ouma, D. Otieno, and C. Mutai, "An ethnobotanical study of medicinal plants used by the Nandi people in Kenya," *Journal of Ethnopharmacology*, vol. 116, no. 2, pp. 370–376, 2008.

[26] G. N. Njoroge and J. W. Kibunga, "Herbal medicine acceptance, sources and utilization for diarrhoea management in a cosmopolitan urban area (Thika, Kenya)," *African Journal of Ecology*, vol. 45, no. s1, pp. 65–70, 2007.

[27] J. K. Mworia, C. M. Kibiti, M. P. Ngugi, and J. N. Ngeranwa, "Antipyretic potential of dichloromethane leaf extract of *Eucalyptus globulus* (Labill) and *Senna didymobotrya* (Fresenius) in rats models," *Heliyon*, vol. 5, no. 12, Article ID e02924, 2019.

[28] C. Ochieng, A. Shrivastava, U. Chaturvedi et al., "Effects of *Senna didymobotrya* root extract and compounds on tritoninduced hyperlipidaemic rats and differentiation of 3T3-Li preadipocytes," *The Natural Products Journal*, vol. 3, no. 3, pp. 212–217, 2013.

[29] S. T. Anthoney, C. N. Mutuku, J. K. Obey, E. Akumu, and E. N. Makau, "Evaluation of in vitro antibacterial activity in Senna didymobotrya roots methanolic-aqua extract and the selected fractions against selected pathogenic microorganisms," *International Journal of Current Microbiology and Applied Sciences*, vol. 3, no. 5, pp. 362–376, 2014.

[30] P. Jeruto, P. F. Arama, B. Anyango, and G. Maroa, "Phytochemical screening and antibacterial investigations of crude methanol extracts of *Senna didymobotrya* (Fresen.) H. S. Irwin & Barneby," *Journal of Applied Biosciences*, vol. 114, no. 1, pp. 11357–11367, 2017.

[31] S. T. Anthoney, K. J. Obey, and C. N. Mutuku, "Assessment of antibacterial activity of hot aqua extract of *Senna didymobotrya* leaves," *Baraton Interdisciplinary Research Journal*, vol. 5, pp. 125–132, 2015.

[32] C. N. Mutuku and H. Ndikiu, "Assessment of antibacterial activity of *Senna didymobotrya* leaves water extract as an alternative remedy to curb nosocomial infections," *International Journal of Bioassays*, vol. 4, no. 4, pp. 3783–3787, 2015.

[33] H. J. Hussein, N. M. Sahi, A. M. Saad, and H. J. Ali Malik Altameme, "The antibacterial effect of bioactive compounds extracted from *Cassia didymobotrya* (fresenius) Irwin & Barne by against some pathogenic bacteria," *Annals of Tropical Medicine and Public Health*, vol. 22, p. SPe117, 2019.

[34] R. K. Korir, C. Mutai, C. Kiiyukia, and C. Bii, "Antimicrobial activity and safety of two medicinal plants traditionally used in bomet district of Kenya," *Research Journal of Medicinal Plant*, vol. 6, no. 5, pp. 370–382, 2012.

[35] J. Mining, Z. O. Lagat, T. Akenga, and P. Tarus, "Bioactive metabolites of *Senna didymobotrya* used as biopesticide against *Acanthoscelides obtectus* in Bungoma, Kenya," *Journal of Applied Pharmaceutical Science*, vol. 4, no. 9, pp. 56–60, 2014.

[36] L. J. McGaw, A. K. Jäger, and J. van Staden, "Antibacterial, anthelmintic and anti-amoebic activity in South African medicinal plants," *Journal of Ethnopharmacology*, vol. 72, no. 1-2, pp. 247–263, 2000.

[37] D. K. Buyela, "Profiling and pathogenicity of *Ralstonia solanacearum* disease of tomato and it's control using *Senna didymobotrya* and *Moringa oleifera* plant extracts in Maseno (Kenya)," MSc thesis, Maseno University, Kisumu, Kenya, 2017.

[38] C. K. Kitonde, D. S. Fidahusein, C. W. Lukhoba, and M. M. Jumba, "Antimicrobial activity and phytochemical screening of *Senna didymobotry* used to treat bacterial and fungal infections in Kenya," *International Journal of Educational Research*, vol. 2, no. 1, pp. 1–12, 2014.

[39] A. M. Madureira, C. Ramalhete, S. Mulhovo, A. Duarte, and M.-J. U. Ferreira, "Antibacterial activity of some African medicinal plants used traditionally against infectious diseases," *Pharmaceutical Biology*, vol. 50, no. 4, pp. 481–489, 2012.

[40] C. M. Ocharo, "Isolation and identification of antibacterial and antifungal compounds from selected Kenyan medicinal plants," MSc thesis, Kenyatta University, Nairobi, Kenya, 2005.

[41] C. A. Orwa and L. G. Njue, "Efficacy of crude extract from candle brush (*Senna didymobotrya*) leaves against *Aspergillus niger* in reduction of post-harvest losses in tomatoes," *Asian Food Science Journal*, vol. 10, no. 2, pp. 1–8, 2019.

[42] O. F. Igunza, J. Ngeranwa, G. Orinda, and P. Mugo, "*In vitro* modulation of clotrimazole, ketoconazole, nystatin, amphotericin B and griseofulvin by *Acmella caulirhiza* and *Senna didymobotrya* extract against Candida spp," *Journal of Applied Biosciences*, vol. 142, pp. 14478–14508, 2019.

[43] L. B. Nyamwamu, M. Ngeiywa, M. Mulaa, A. Lelo, J. Ingonga, and A. Kimutai, "Acute toxicity of *Senna didymobotrya* fresen irwin roots used as a traditional medicinal plant in Kenya," *American International Journal of Contemporary Research*, vol. 5, no. 4, pp. 74–77, 2015.

[44] G. J. Maina, T. Maitho, and J. M. Mbaria, "Antifleas activity and safety of *Tithonia diversifolia* and *Senna didymobotrya* extracts," *Journal of Pharmacy and Pharmacology Research*, vol. 2, no. 3, pp. 78–92, 2018.

[45] I. Alemayehu, S. Tadesse, F. Mammo, B. Kibret, and M. Endale, "Phytochemical analysis of the roots of *Senna didymobotrya*," *Journal of Medicinal Plants Research*, vol. 9, no. 34, pp. 900–907, 2015.

[46] L. P. Maema, M. Potgieter, N. A. Masevhe, and A. Samie, "Antimicrobial activity of selected plants against fungal species isolated from South African AIDS patients and their antigonococcal activity," *Journal of Complementary & Integrative Medicine*, vol. 17, no. 3, Article ID 20190087, 2020.

[47] S. Biswas, S. Chakraborty, and A. F. Mulaba-Bafubiandi, "Optimization of copper nanoparticle biosynthesis process using aqueous extract of *Andrographis paniculata*," *African Journal of Science, Technology, Innovation and Development*, vol. 9, no. 1, pp. 131–138, 2017.

[48] M. Asemani and N. Anarjan, "Green synthesis of copper oxide nanoparticles using *Juglans regia* leaf extract and assessment of their physico-chemical and biological properties," *Green Processing and Synthesis*, vol. 8, no. 1, pp. 557–567, 2019.

[49] E. V. Kigondu, G. M. Rukunga, J. M. Kerik et al., "Antiparasitic activity and cytotoxicity of selected medicinal plants from Kenya," *Journal of Ethnopharmacology*, vol. 123, pp. 504–509, 2009.

[50] T. Omara, A. K. Kiprop, and V. J. Kosgei, "Intraspecific variation of phytochemicals, antioxidant, and antibacterial activities of different solvent extracts of *Albizia coriaria* leaves from some agroecological zones of Uganda," *Evidence-based Complementary and Alternative Medicine*, vol. 2021, Article ID 2335454, 14 pages, 2021.

[51] H. Barabadi, S. Honary, P. Ebrahimi, M. A. Mohammadi, A. Alizadeh, and F. Naghibi, "Microbial mediated preparation, characterization and optimization of gold

nanoparticles," *Brazilian Journal of Microbiology*, vol. 45, no. 4, pp. 1493–1501, 2015.

[52] N. Krithiga, A. Jayachitra, and A. Rajalakshmi, "Synthesis, characterization and analysis of the effect of copper oxide nanoparticles in biological systems," *Indian Journal of NanoScience*, vol. 1, pp. 6–15, 2013.

[53] P. Prema, "Chemical mediated synthesis of silver nanoparticles and its potential antibacterial application," in *Progress in Molecular and Environmental Bioengineering–from Analysis and Modeling to Technology Applications*, pp. 151–166, IntechOpen, London, UK, 2010.

[54] J. Hudzicki, *Kirby-Bauer Diffusion Susceptibility Test Protocol*, American Society for Microbiology (ASM), Washington, DC, USA, 2009.

[55] Clinical Laboratory Standards Institute, "Performance standards for antimicrobial disk susceptibility tests; Approved standard," Clinical Laboratory Standards Institute, Wayne, PA, USA, 9th edition, 2010.

[56] M. Nasrollahzadeh, Z. Issaabadi, and S. M. Sajadi, "Green synthesis of a Cu/MgO nanocomposite by *Cassytha filiformis* L. extract and investigation of its catalytic activity in the reduction of methylene blue, congo red and nitro compounds in aqueous media," *RSC Advances*, vol. 8, no. 7, pp. 3723–3735, 2018.

[57] G. Rajagopal, A. Nivetha, M. Sundar et al., "Mixed phytochemicals mediated synthesis of copper nanoparticles for anticancer and larvicidal applications," *Heliyon*, vol. 7, no. 6, Article ID e07360, 2021.

[58] B. K. Sharma, D. V. Shah, and D. R. Roy, "Green synthesis of CuO nanoparticles using *Azadirachta indica* and its antibacterial activity for medicinal applications," *Materials Research Express*, vol. 5, no. 9, Article ID 095033, 2018.

[59] D. Kalaimurugan, P. Sivasankar, K. Lavanya, M. S. Shivakumar, and S. Venkatesan, "Antibacterial and larvicidal activity of *Fusarium proliferatum* (YNS2) whole cell biomass mediated copper nanoparticles," *Journal of Cluster Science*, vol. 30, no. 4, pp. 1071–1080, 2019.

[60] A. Y. Ghidan, T. M. Al-Antary, and A. M. Awwad, "Green synthesis of copper oxide nanoparticles using *Punica granatum* peels extract: effect on green peach aphid," *Environmental Nanotechnology, Monitoring & Management*, vol. 6, pp. 95–98, 2016.

[61] S. Vasantharaj, S. Sathiyavimal, M. Saravana et al., "Synthesis of ecofriendly copper oxide nanoparticles for fabrication over textile fabrics: characterization of antibacterial activity and dye degradation potential," *Journal of Photochemistry and Photobiology B: Biology*, vol. 191, pp. 143–149, 2019.

[62] T. M. D. Dang, T. T. T. Le, E. Fribourg-Blanc, and M. C. Dang, "Synthesis and optical properties of copper nanoparticles prepared by a chemical reduction method," *Advances in Natural Sciences: Nanoscience and Nanotechnology*, vol. 2, no. 1, Article ID 015009, 2011.

[63] O. O. Ogundipe, J. O. Moody, P. J. Houghton, and H. A. Odelola, "Bioactive chemical constituents from *Alchornea laxiflora* (benth) pax and hoffman," *Journal of Ethnopharmacology*, vol. 74, no. 3, pp. 275–280, 2001.

[64] M. Nasrollahzadeh and S. Mohammad Sajadi, "Green synthesis of copper nanoparticles using *Ginkgo biloba* L. leaf extract and their catalytic activity for the Huisgen [3 + 2] cycloaddition of azides and alkynes at room temperature," *Journal of Colloid and Interface Science*, vol. 457, pp. 141–147, 2015.

[65] I. DeAlba-Montero, J. Guajardo-Pacheco, E. Morales-Sánchez et al., "Antimicrobial properties of copper nanoparticles and amino acid chelated copper nanoparticles produced by using a soya extract," *Bioinorganic Chemistry and Applications*, vol. 2017, Article ID 1064918, 6 pages, 2017.

[66] J. Ramyadevi, K. Jeyasubramanian, A. Marikani, G. Rajakumar, and A. A. Rahuman, "Synthesis and antimicrobial activity of copper nanoparticles," *Materials Letters*, vol. 71, pp. 114–116, 2012.

[67] G. H. Chan, J. Zhao, E. M. Hicks, G. C. Schatz, and R. P. Van Duyne, "Plasmonic properties of copper nanoparticles fabricated by nanosphere lithography," *Nano Letters*, vol. 7, no. 7, pp. 1947–1952, 2007.

[68] R. Liu, H. Zhang, and R. Lal, "Effects of stabilized nanoparticles of copper, zinc, manganese, and iron oxides in low concentrations on lettuce (*Lactuca sativa*) seed germination: nanotoxicants or nanonutrients?" *Water, Air, & Soil Pollution*, vol. 227, no. 1, p. 42, 2016.

[69] A. Tamilvanan, K. Balamurugan, T. Mohanraj, P. Selvakumar, and B. Madhankumar, "Parameter optimization of copper nanoparticle synthesis by electrodeposition process using RSM and CS," *Materials Today: Proceedings*, vol. 45, no. 2, pp. 751–756, 2021.

[70] S. Honary, H. Barabadi, F. Gharaeifathabad, and F. Naghibi, "Green synthesis of copper oxide nanoparticles using *Penicillium aurantiogriseum*, *Penicillium citrinum* and *Penicillium waksmanii*," *Digest Journal of Nanomaterials and Biostructures*, vol. 7, pp. 999–1005, 2012.

[71] O. N. Erick and M. P. Nalini, "Green chemistry focus on optimization of silver nanoparticles using response surface methodology (RSM) and mosquitocidal activity: *Anopheles stephensi* (Diptera: Culicidae)," *Spectrochimica Acta Part A Molecular and Biomolecular Spectroscopy*, vol. 149, pp. 978–984, 2015.

[72] H.-X. Zhang, U. Siegert, R. Liu, and W.-B. Cai, "Facile fabrication of ultrafine copper nanoparticles in organic solvent," *Nanoscale Research Letters*, vol. 4, no. 7, p. 705, 2009.

[73] B. K. Park, D. Kim, S. Jeong, J. Moon, and J. S. Kim, "Direct writing of copper conductive patterns by ink-jet printing," *Thin Solid Films*, vol. 515, no. 19, pp. 7706–7711, 2007.

[74] R. Sankar, R. Maheswari, S. Karthik, K. S. Shivashangari, and V. Ravikumar, "Anticancer activity of Ficus religiosa engineered copper oxide nanoparticles," *Materials Science and Engineering: C*, vol. 44, pp. 234–239, 2014.

[75] B. Salopek, D. Krasic, and S. Filipovic, "Measurement and application of zeta-potential," *Rudarsko-Geolosko-Naftni Zbornik*, vol. 4, p. 147, 1992.

[76] J. Karimi and S. Mohsenzadeh, "Rapid, green, and ecofriendly biosynthesis of copper nanoparticles using flower extract of aloe vera," *Synthesis and Reactivity in Inorganic Metal-Organic and Nano-Metal Chemistry*, vol. 45, no. 6, pp. 895–898, 2015.

[77] S. Saif, A. Tahir, T. Asim, and Y. Chen, "Plant mediated green synthesis of CuO nanoparticles: comparison of toxicity of engineered and plant mediated CuO nanoparticles towards *Daphnia magna*," *Nanomaterials*, vol. 6, no. 11, p. 205, 2016.

[78] M. S. Usman, M. E. El Zowalaty, K. Shameli, N Zainuddin, M Salama, and N. A Ibrahim, "Synthesis, characterization, and antimicrobial properties of copper nanoparticles," *International Journal of Nanomedicine*, vol. 8, pp. 4467–4479, 2013.

[79] H.-f. Chen, J.-j. Wu, M.-y. Wu, and H. Jia, "Preparation and antibacterial activities of copper nanoparticles encapsulated by carbon," *New Carbon Materials*, vol. 34, no. 4, pp. 382–389, 2019.

[80] T. J. Silhavy, D. Kahne, and S. Walker, "The bacterial cell envelope," *Cold Spring Harbor perspectives in biology*, vol. 2, no. 5, Article ID a000414, 2010.

[81] M. J. Hajipour, K. M. Fromm, A. Ashkarran et al., "Antibacterial properties of nanoparticles," *Trends in Biotechnology*, vol. 30, no. 10, pp. 499–511, 2012.

[82] M. Raffi, S. Mehrwan, T. M. Bhatti et al., "Investigations into the antibacterial behavior of copper nanoparticles against *Escherichia coli*," *Annals of Microbiology*, vol. 60, no. 1, pp. 75–80, 2010.

[83] S. L. Warnes and C. W. Keevil, "Mechanism of copper surface toxicity in vancomycin-resistant enterococci following wet or dry surface contact," *Applied and Environmental Microbiology*, vol. 77, no. 17, pp. 6049–6059, 2011.